

Potent Antitumor Activity of MS-247, a Novel DNA Minor Groove Binder, Evaluated by an *in Vitro* and *in Vivo* Human Cancer Cell Line Panel¹

Takao Yamori,² Akio Matsunaga, Shigeo Sato, Kanami Yamazaki, Akiko Komi, Kazuhiro Ishizu, Izumi Mita, Hajime Edatsugi, Yasuhiro Matsuba, Kimiko Takezawa, Osamu Nakanishi, Hiroshi Kohno, Yuki Nakajima, Hironori Komatsu, Toshio Andoh, and Takashi Tsuruo

Division of Experimental Chemotherapy, Cancer Chemotherapy Center, Japanese Foundation for Cancer Research, Tokyo 170-8455 [T. Y., S. S., K. Y., A. K., K. I.]; Life Sciences Laboratory, Mitsui Chemical Inc., Chiba 297-0017 [A. M., H. K., Y. N., H. K.]; Institute of Biological Science, Mitsui Pharmaceuticals, Inc., Chiba 297-0017 [I. M., H. E., Y. M., K. T., O. N.]; Faculty of Engineering, Soka University, Tokyo 192-0003 [T. A.]; and Institute of Molecular and Cellular Biosciences, University of Tokyo, Tokyo 113-0032 [T. T.], Japan

ABSTRACT

We synthesized a novel anticancer agent MS-247 (2-[[N-[1-methyl-2-[5-[N-[4-[N,N-bis(2-chloroethyl) amino] phenyl]] carbamoyl]-1H-benzimidazol-2-yl] pyrrol-4-yl] carbamoyl] ethyldimethylsulfonium di-*p*-toluenesulfonate) that has a netropsin-like moiety and an alkylating residue in the structure. We evaluated antitumor activity of MS-247 using a human cancer cell line panel coupled with a drug sensitivity database and subsequently using human cancer xenografts. The average MS-247 concentration required for 50% growth inhibition against a panel of 39 cell lines was 0.71 μ M. The COMPARE analysis revealed that the differential growth inhibition pattern of MS-247 significantly correlated with those of camptothecin analogues and anthracyclins, indicating that MS-247 and the two drug groups might have similar modes of action. MS-247 exhibited remarkable antitumor activity against various xenografts. A single i.v. injection of MS-247 significantly inhibited the growth of all 17 xenografts tested, which included lung, colon, stomach, breast, and ovarian cancers. In many cases, MS-247 was more efficacious than cisplatin, Adriamycin, 5-fluorouracil, cyclophosphamide, VP-16, and vincristine and was almost comparable with paclitaxel and CPT-11; these are the most clinically promising drugs at present. MS-247 was noticeably more effective than paclitaxel (in HCT-15) and CPT-11 (in A549, HBC-4, and SK-OV-3). The toxicity of MS-247, indicated by body weight loss, was reversible within 10 days after administration. The MS-247 mode of action showed DNA binding activity at the site where Hoechst 33342 bound, inhibited topoisomerases I and II (as expected by the COMPARE analysis) blocked the cell cycle at the G₂-M phase, and induced apoptosis. These results indicate that MS-247 is a promising new anticancer drug candidate to be developed further toward clinical trials.

INTRODUCTION

DNA minor groove binders are an attractive source of novel antitumor agents. As a whole, they induce a huge range of mutations from simple base sequence changes to deletions and ploidy changes (reviewed in Ref. 1). The recent increased interest in this group of compounds stems from their ability to interact in a sequence-selective fashion at quite long DNA binding sites, suggesting the possibility of targeting specific DNA sequences within the genome (2–6). Several DNA minor groove binders proved to have potent antitumor activity in preclinical studies and are now under clinical phase studies. They include duocarmycin derivatives adozelesin (7–9), carzelesin (10, 11), bizelesin (12, 13) and KW-2189 (14), and a distamycin A-derivative tallimustine (15). However, their clinical efficacies have not been established yet (16–19).

Received 3/23/99; accepted 6/8/99.

The costs of publication of this article were defrayed in part by the payment of page charges. This article must therefore be hereby marked *advertisement* in accordance with 18 U.S.C. Section 1734 solely to indicate this fact.

¹ This work was supported in part by a Grant-in-Aid for Scientific Research on Priority Area "Cancer" from the Ministry of Education, Science, Sports and Culture, Japan, as well as by a grant from the Organization for Pharmaceutical Safety and Research of Japan.

² To whom requests for reprints should be addressed, at Cancer Chemotherapy Center, Japanese Foundation for Cancer Research, 1-37-1 Kami-Ikebukuro, Toshima-ku, Tokyo 170-8455, Japan. Phone: 81-3-3918-0111, extension 4453; Fax: 81-3-3918-3716.

We attempted to develop a new DNA minor groove binder that has the more promising antitumor activity. We synthesized compounds that have two moieties in the structure. One is a netropsin-like moiety (Fig. 1) to acquire DNA minor groove binding activity, and another is an *N,N*-bis(2-chloroethyl) amino residue for DNA alkylation. Netropsin is one of the polypyrrolicarboxamides, like distamycin A, and binds to DNA minor grooves at the A-T-rich region (20). After screening a number of synthetic compounds, we selected MS-247³ (Fig. 1). It had shown significant cytotoxicity in several murine tumor cell lines and strong *in vivo* antitumor activity against murine tumor models in our preliminary study.

The present study was designed to evaluate the antitumor activity of MS-247 against various human cancers *in vitro* and *in vivo* and to elucidate its mode of action. We report here that MS-247 indicated potent antitumor activity against all 17 human xenografts tested, and that MS-247 bound to the DNA minor groove, inhibited topoisomerases I and II, blocked the cell cycle at G₂-M phase, and induced apoptosis.

MATERIALS AND METHODS

Chemicals. MS-247 was synthesized in the Life Sciences Laboratory Mitsui Chemicals, Inc. (Chiba, Japan). MS-247 was dissolved in *N,N*-dimethylformamide (Tokyo Kasei Kogyo, Tokyo, Japan) before use. CPT-11 was kindly supplied by Yakult Honsha (Tokyo, Japan). Other anticancer drugs and chemicals were purchased as follows: ADM and 5-FU, Kyowa Hakkō Kogyo (Tokyo, Japan); cisplatin and VP-16, Nippon Kayaku (Tokyo, Japan); CPM, Shionogi Pharmaceuticals (Osaka, Japan); VCR, Eli Lilly Japan (Kobe, Japan); paclitaxel, camptothecin, calf thymus DNA, RNase A, and propidium iodide, Sigma (St. Louis, MO.); Hoechst 33342, Molecular Probes (Eugene, OR); Proteinase K, Boehringer Mannheim (Mannheim, Germany); and ϕ X174/*Hae*III, Toyobo (Tokyo, Japan).

Cell Lines. Human breast cancer MDA-MB-231 and leukemia HL-60 were purchased from American Type Culture Collection (Rockville, MD). Murine leukemia L1210, P388, and the following human cancer cell lines (21) were generously distributed by the National Cancer Institute (Frederick, MD): lung cancer, NCI-H23, NCI-H226, NCI-H522, NCI-H460, DMS273 and DMS114; colon cancer, HCC-2998, KM-12, HT-29, WiDr, HCT-15, and HCT-116; ovarian cancer, OVCAR-3, OVCAR-4, OVCAR-5, OVCAR-8, and SK-OV-3; breast cancer, MCF-7; renal cancer, RXF-631 L and ACHN; melanoma, LOX-IMVI; and brain tumor, U251, SF-295, SF-539, SF-268, SNB-75, and SNB-78. Human stomach cancer, MKN-1, MKN-7, MKN-28, MKN-45, MKN-74, and St-4, and human breast cancer BSY-1, HBC-4, and HBC-5 were described elsewhere (22, 23). The cells were cultured in RPMI 1640 supplemented with 5% fetal bovine serum, penicillin (100 units/ml), and streptomycin (100 mg/ml) at 37°C in humidified air containing 5% CO₂.

A Human Cancer Cell Line Panel and the Database. To evaluate drugs for the cell growth inhibition profile, we established a human cancer cell line

³ The abbreviations used are: MS-247, 2-[[N-[1-methyl-2-[5-[N-[4-[N,N-bis(2-chloroethyl) amino] phenyl]] carbamoyl]-1H-benzimidazol-2-yl] pyrrol-4-yl] carbamoyl] ethyldimethylsulfonium di-*p*-toluenesulfonate; ADM, Adriamycin; 5-FU, 5-fluorouracil; CPM, cyclophosphamide; VCR, vincristine; VP-16, etoposide; GI₅₀, concentration required for 50% growth inhibition; PBS(-), calcium- and magnesium-free PBS.

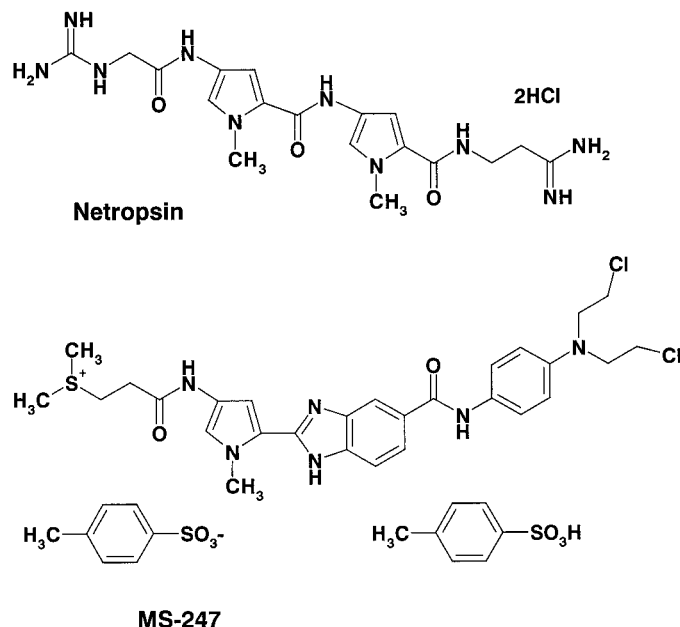


Fig. 1. Chemical structure of netropsin and MS-247. MS-247 has a netropsin-like moiety and an alkylating residue in the structure.

panel combined with a database. The system as a whole was developed according to the method of the National Cancer Institute (24–26), with modification. The cell line panel consisted of 38 human cancer cell lines, described above, and 1 murine leukemia (P388). With this system, we have examined the antiproliferative effect of more than 200 standard compounds, including various anticancer drugs, and established a new database, as described below.

Measurements of Cell Growth Inhibition and Data Analysis. The details of measuring cell growth inhibition are described elsewhere (26, 27). Briefly, the cells were plated at proper density in 96-well plates in RPMI 1640 with 5% fetal bovine serum and allowed to attach overnight. The cells were exposed to drugs for 48 h. Then, the cell growth was determined according to the sulforhodamine B assay, described by Skehan *et al.* (28). Data calculations were made according to the method described previously (26). Absorbance for the control well (C) and the tests well (T) were measured at 525 nm. Moreover, at time 0 (addition of drugs), absorbance for the test well (T_0) was also measured. Using these measurements, cell growth inhibition (percentage of growth) by each concentration of drug was calculated as: % growth = $100 \times [(T - T_0)/(C - T_0)]$, when $T > T_0$ and % growth = $100 \times [(T - T_0)/T]$, when $T < T_0$. By using the computer to process % growth values, the 50% growth inhibition parameter (GI_{50}) was determined. The GI_{50} was calculated as $100 \times [(T - T_0)/(C - T_0)] = 50$. The mean graph, which shows the differential growth inhibition of the drug in the cell line panel, was drawn based on a calculation using a set of GI_{50} (24, 25). To analyze the correlation between the mean graphs of drug A and drug B, the COMPARE computer algorithm was developed according to the method described by Paull *et al.* (25). Pearson correlation coefficients were calculated using the following formula: $r = (\sum(x_i - x_m)(y_i - y_m))/(\sum(x_i - x_m)^2 \sum(y_i - y_m)^2)^{1/2}$, where x_i and y_i are log GI_{50} of drug A and drug B, respectively, against each cell line, and x_m and y_m are the mean values of x_i and y_i , respectively.

Animals. Female nude mice with BALB/c genetic backgrounds were purchased from Charles River Japan, Inc. (Kanagawa, Japan). They were maintained under specific pathogen-free conditions and provided with sterile food and water *ad libitum*. Seven-week-old mice weighing 16–22 g were used for this study.

Drugs and Administration. Drug administration was done *i.v.* We selected an administration schedule of single shot for MS-247, according to the results in animal tumor models.⁴ We first determined the maximum tolerable dose of MS-247 in the schedule, which was 30 mg/kg. To evaluate the

antitumor effect, MS-247 was given to tumor-bearing nude mice at doses of 30, 25, and 21 mg/kg for lung cancer xenografts and at a dose of 25 mg/kg for other xenografts. The reference drugs chosen were CPT-11, paclitaxel, cisplatin, ADM, 5-FU, CPM, VP-16, and VCR. Each reference drug was given at the maximum tolerable dose in the optimal schedule.

Antitumor Activity against Xenografts. Six lung cancers (NCI-H23, NCI-H226, NCI-H460, A549, DMS114, and DMS273), four stomach cancers (MKN-1, MKN-7, MKN-74, and St-4), three colon cancers (HCC-2998, HCT-116, and HCT-15), two breast cancers (HBC-4 and MDA-MB-231), and two ovarian cancers (SK-OV-3 and OVCAR-8) were used to evaluate antitumor activity of MS-247. They were grown as *s.c.* tumors in nude mice. Nude mice were inoculated *s.c.* with a $3 \times 3 \times 3$ -mm tumor fragment. When the tumor reached 100–300 mm³ in volume, animals were divided randomly into test groups consisting of six mice per group (day 0). Drugs were administered from day 0 according to the dose schedules indicated. The mice were weighed twice each week up to days 24–31 to monitor the toxic effects. The length (L) and width (W) of the tumor mass were measured twice a week up to days 24–31, and the tumor volume (TV) was calculated as: $TV = (L \times W^2)/2$. The tumor volume at day n was expressed as relative tumor volume (RTV), according to the following formula: $RTV = TV_n/TV_0$, where TV_n is the tumor volume at day n , and TV_0 is the tumor volume at day 0. Tumor regression ($T/C\%$) on day 14 was determined by calculating RTV as: $T/C\% = 100 \times (\text{mean } RTV \text{ of treated group})/(\text{mean } RTV \text{ of control group})$. Statistical evaluations of RTV were performed using the Mann-Whitney U test.

Measurement of Fluorescence of DNA-bound Hoechst 33342. In the cell free system, 1 μg of calf thymus DNA and 0.8 μg of Hoechst 33342 were mixed in 0.2 ml of PBS(–) and preincubated for 10 min at room temperature in a 96-well plate. Then, MS-247 was added at final concentrations of 0.01–30 $\mu\text{g}/\text{ml}$. After another 10-min incubation, the fluorescence derived from the Hoechst 33342 bound to DNA was measured with a fluorometer (excitation wavelength, 355 nm; and emission wavelength, 460 nm). In the cellular system, L1210 cells (4×10^5 cells in 1 ml of culture medium) were preincubated with Hoechst 33342 (4 $\mu\text{g}/\text{ml}$) at 37°C for 20 min. Then, MS-247 was added at final concentrations of 0.01–100 $\mu\text{g}/\text{ml}$. After another 20-min incubation, the cells were washed once with ice-cold PBS(–), resuspended in ice-cold PBS(–), and transferred into a 96-well plate. Fluorescence was measured as described above.

Cell Cycle Analysis. Cell cycle analysis was performed using flow cytometry, as described previously (29). The L1210 cells were exposed to MS-247 for 3–48 h. The cells were harvested, washed with ice-cold PBS(–), and fixed in 70% ethanol. The cells were washed twice with ice-cold PBS(–) again, treated with RNase (0.25 $\mu\text{g}/\text{ml}$) at 37°C for 1 h, and stained with propidium iodide (50 $\mu\text{g}/\text{ml}$). The DNA content of the cells was analyzed using an EPICS ELITE flow cytometer (Coulter, Hialeah, FL).

Topoisomerase Activity Assays. Topoisomerase I enzyme activity was measured by DNA relaxation assay using the Topoisomerase I Drug Screening kit (TopoGEN, Columbus, OH). Briefly, supercoiled DNA (0.25 μg) was suspended in a standard reaction mixture [10 mM Tris-HCl (pH 7.9), 1 mM EDTA, 150 mM NaCl, 0.1% BSA, 0.1 mM spermidine, and 5% glycerol]. MS-247 was added to the mixture before the reaction was started by topoisomerase I enzyme addition. After a 30-min incubation at 37°C, the reaction was stopped by adding 0.1 volume of 10% SDS. The DNA-bound protein (topoisomerase I) was digested by proteinase K (41.7 $\mu\text{g}/\text{ml}$) at 37°C for 30 min. The proteinase K was removed by chloroform:isoamylalcohol (24:1, v/v) treatment. DNA samples were then analyzed by 1% agarose gel electrophoresis.

DNA Fragmentation Assay. DNA fragmentation was analyzed by agarose gel electrophoresis. The HL-60 cells (5×10^5) were treated with 0.2 or 2 μM MS-247 or 20 nM camptothecin at 37°C for 20 h. The drug-treated cells were harvested and then suspended in TNE buffer [10 mM Tris-HCl (pH 7.6), 140 mM NaCl, and 1 mM EDTA]. Subsequently, it was lysed by incubation at 37°C for 30 min in the TNE buffer containing 0.2 mg/ml of RNase A, 0.2 mg/ml of Proteinase K, and 0.83% SDS. DNA extraction was performed as described previously (30), and extracted DNA was resuspended in TNE buffer, then treated with RNase A (0.2 mg/ml) at 37°C for 30 min, after Proteinase K (0.2 mg/ml) digestion at 37°C for 30 min. The purified DNA was resolved by electrophoresis in 2% agarose gels, stained with ethidium bromide, and visualized under UV light.

⁴ Unpublished results.

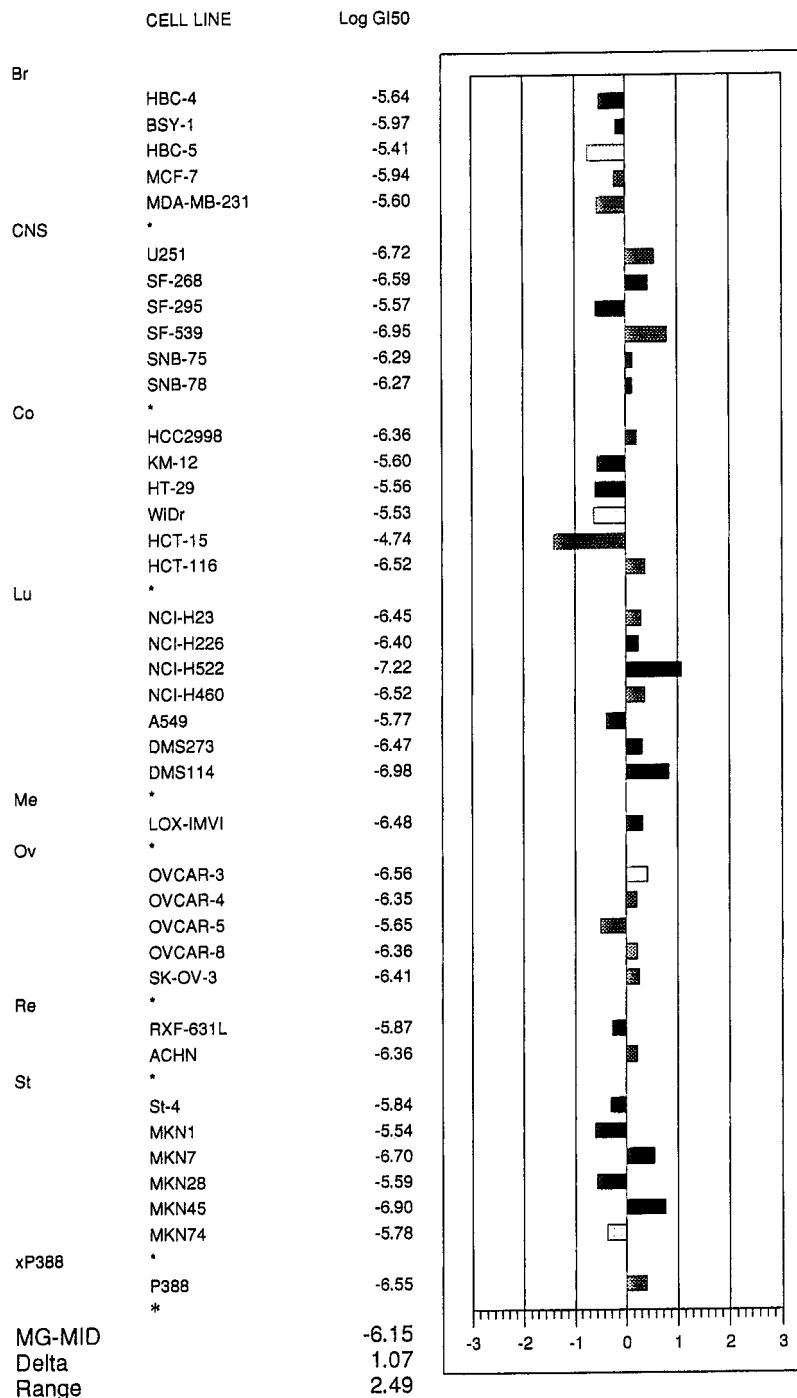


Fig. 2. Growth inhibition against a panel of 38 human cancer cell lines. The mean graph was produced by computer processing of the GI₅₀s as described in "Materials and Methods." The log GI₅₀ for each cell line is indicated. Columns extending to the right, sensitivity to MS-247; columns extending to the left, resistance to MS-247. One scale represents one logarithm difference. MG-MID, the mean of log GI₅₀ values for 39 cell lines. Delta, the logarithm of difference between the MG-MID and the log GI₅₀ of the most sensitive cell line. Range, the logarithm of difference between the log GI₅₀ of the most resistant cell line and the log GI₅₀ of the most sensitive one.

RESULTS

Growth Inhibition against a Panel of 38 Human Cancer Cell Lines. We have established a new human cancer cell line panel coupled with a drug sensitivity database, which is similar to the one developed by the National Cancer Institute (24–26). This panel consists of 38 human cancer cell lines and murine leukemia P388. Thus far, we have used this panel to evaluate more than 200 standard agents, most of which are anticancer drugs and various types of inhibitors. We have also added the growth-inhibitory parameters to the database. We compared standard drugs with each other for the mean graph pattern using COMPARE analysis and confirmed that drugs sharing a certain mode of action clustered together, as described

previously (24, 25). The patterns in the mean graphs of drugs with common modes of action resembled one another.

Using the human cancer cell line panel, we investigated the cell growth inhibition profile of MS-247. Fig. 2 shows the mean graph of MS-247 based on the growth inhibition parameter of GI₅₀. MS-247 showed differential growth inhibition, and it seemed to be more effective against lung cancer cell lines. The mean log GI₅₀ of MS-247 was -6.15 (0.71 μM), which fell in the middle of the range of presently used anticancer drugs in the panel (Fig. 3). The COMPARE analysis of the mean graph revealed that MS-247 significantly correlated with two main groups of anticancer agents (Table 1). The first was a camptothecin analogue group, including CPT-11, SN-38 (active

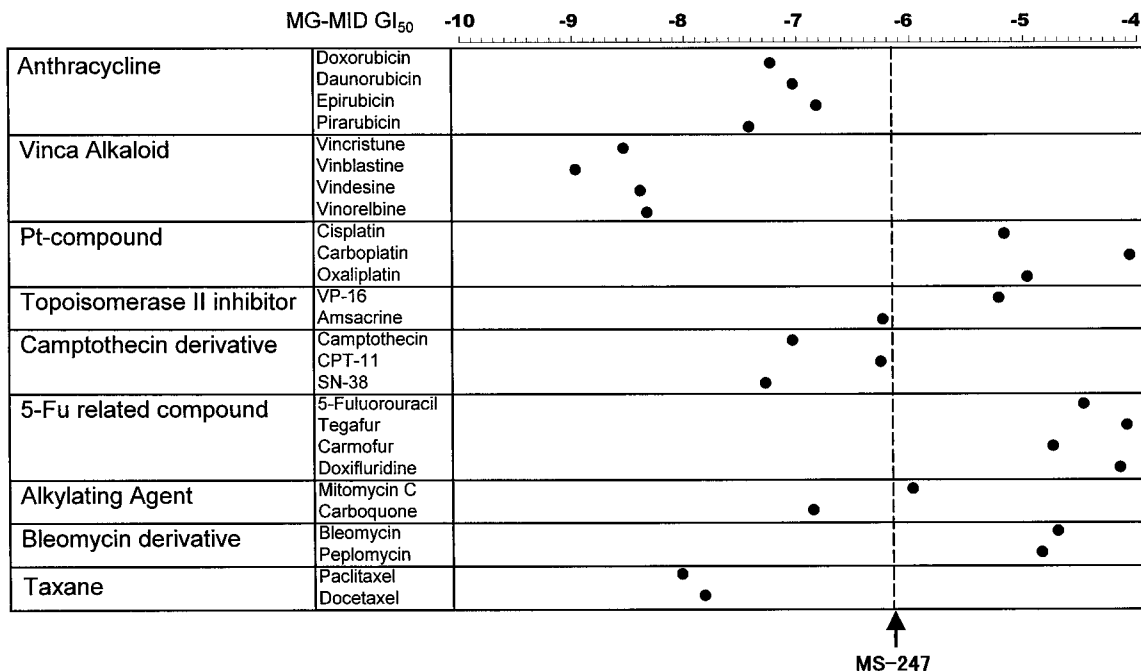


Fig. 3. Comparison of MS-247 with clinically active anticancer agents for the mean log GI₅₀ against 39 cell lines. The GI₅₀ of each drug to 39 cell lines was determined as described in "Materials and Methods." ●, mean log GI₅₀ of each drug.

metabolite of CPT-11), and camptothecin. The second was an anthracyclin group, including epirubicin, ADM, mitoxantrone, KW-2170, and daunorubicin. These results indicate that MS-247 may share some modes of action with both groups.

Antitumor Activity of MS-247 against Human Cancer Xenografts. To evaluate the antitumor activity of MS-247, we developed various human cancer xenografts by s.c. injecting 17 cell lines of the panel into nude mice. We examined the antitumor activity and the toxicity of MS-247 using six lung cancer xenografts (Fig. 4). The four lung cancer cell lines, NCI-H23, NCI-H226, NCI-H460, and A549, were originally non-small cell lung cancers, and others, DMS273 and DMS114, were small cell lung cancers. A single i.v. administration of MS-247 on day 0 significantly inhibited tumor growth at all of the dosages, 30, 25, and 21 mg/kg (Fig. 4, upper panels). There were not major differences in the efficacy within a dose range, indicating that MS-247 was effective in a rather wide dose range. It is remarkable that MS-247 induced tumor regression during a certain period in NCI-H23, NCI-H226, DMS273, and DMS114. As for toxicity, the body weight of the tumor-bearing mice decreased by day 10 after the administration, but it was recovered afterward (Fig. 4, lower panels). These results demonstrated the therapeutic efficacy of MS-247 in the nude mice bearing lung cancer xenografts.

Then, we examined MS-247 for activity against 10 other xenografts including colon, stomach, breast, and ovarian cancers, and we compared MS-247 with eight major anticancer drugs, paclitaxel, CPT-11, cisplatin, ADM, 5-FU, CPM, VP-16, and VCR (Table 2). A single injection of 25 mg/kg MS-247 showed significant antitumor activity against all 17 xenografts tested. MS-247 was more effective in most xenografts than cisplatin, ADM, 5-FU, CPM, VP-16, or VCR. MS-247 was comparable to paclitaxel and CPT-11, presently the most promising drugs. Noticeably, MS-247 was more effective than paclitaxel in HCT-15 and than CPT-11 in A549, HBC-4, and SK-OV-3; therefore, it showed a higher response rate than paclitaxel and CPT-11.

DNA Binding of MS-247. Hoechst 33342 is a fluorochrome that binds to the DNA minor groove and generates specific fluorescence

(31, 32). To confirm MS-247 binding to DNA, we observed the effect of MS-247 on the fluorescence generated by DNA-bound Hoechst 33342. In a cell free system, the fluorescence of DNA-bound Hoechst 33342 was quenched after MS-247 was added in a dose-dependent manner (Fig. 5A). Similar results were obtained when fluorescence was measured in the cellular system where MS-247 was exogenously added to L1210 cells that had been preincubated with Hoechst 33342 (Fig. 5B). These results indicated that MS-247 may have displaced the DNA-bound Hoechst 33342 on the DNA.

Inhibition of Topoisomerase I by MS-247. Some of the DNA minor groove binders reportedly inhibit topoisomerases (1). In addition, the COMPARE analysis of the mean graph of MS-247 suggested that the mode of action of MS-247 was similar to camptothecin analogues and anthracyclins, which inhibit topoisomerases I and II, respectively. Therefore, we examined whether MS-247 inhibited topoisomerases (Fig. 6). Topoisomerase I converted supercoiled DNA to nicked and relaxed DNA. MS-247 inhibited the process in a dose-dependent manner. These results demonstrated that MS-247 had topoisomerase I inhibitory activity at concentrations of 50–100 μg/ml. MS-247 also inhibited topoisomerase II activity at the same concentration range (data not shown).

Table 1 The COMPARE analysis of MS-247

The mean graph of MS-247 was compared with those of 200 standard compounds using the COMPARE analysis. Drugs were ordered according to the correlation coefficient. Drugs with correlation coefficients higher than 0.5 (P < 0.001) were included.

Ranking order	Drug	r ^a
1	SN-38	0.688
2	CPT-11	0.683
3	Epirubicin	0.636
4	ADM	0.602
5	Mitoxantrone	0.596
6	KW2170	0.588
7	Melphalan	0.579
8	DMDC	0.575
9	Camptothecin	0.557
10	Daunorubicin	0.516

^a Pearson correlation coefficient.

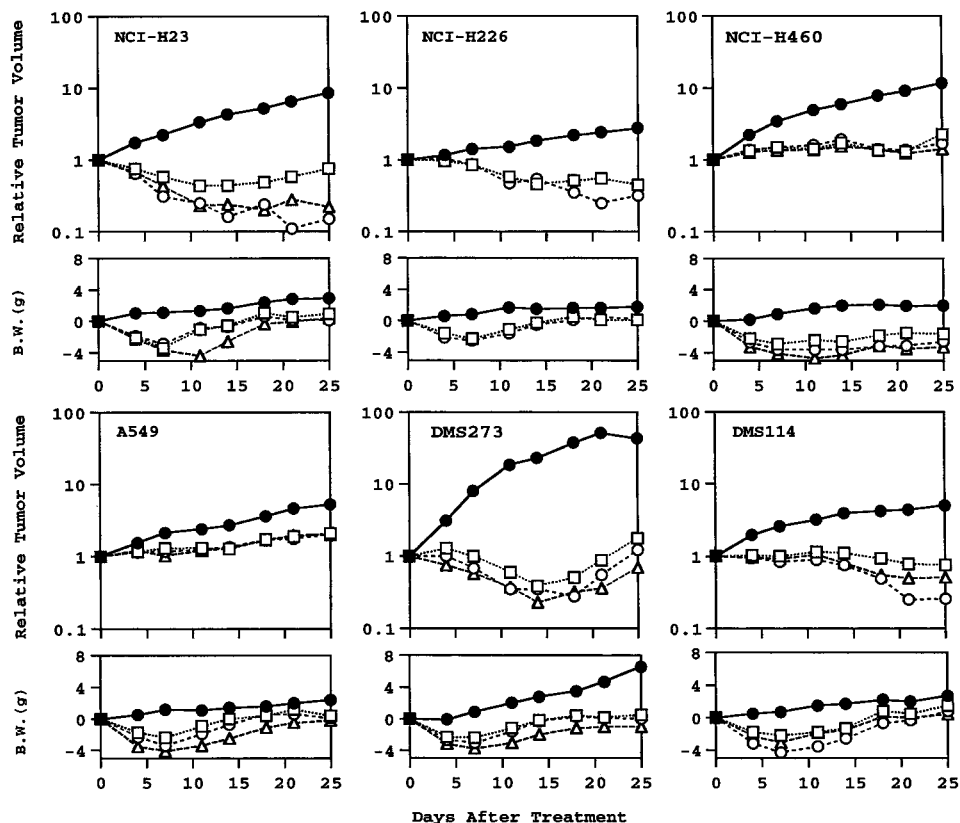


Fig. 4. Effect of MS-247 on the tumor growth and the body weight change in nude mice bearing human lung cancer xenografts. Tumor inoculation was carried out as described in "Materials and Methods." MS-247 was administered on day 0 at doses of 30 (Δ), 25 (\circ), 21 (\square), and 0 mg/kg (\bullet , control). Each curve represents the average of six mice.

Effects of MS-247 on the Cell Cycle. We investigated the effect of MS-247 on cell cycle progression in L1210 cells (Fig. 7). The cells were exposed to 10, 30, and 100 ng/ml of MS-247 for 3–48 h. The cell population in G_2 -M phase increased time dependently at each con-

centration, indicating that MS-247 blocked the cell cycle at the G_2 -M phase.

Apoptosis Induced by MS-247. We tested the apoptosis-inducing ability of MS-247 in HL-60 cells by DNA fragmentation assay. As

Table 2 Antitumor activity of MS-247 against human cancer xenografts

Nude mice were each inoculated s.c. with a $3 \times 3 \times 3$ -mm tumor fragment. When tumors reached 100–300 mm³ in volume, animals were divided randomly into test groups of six each (day 0). Drugs were administered from day 0 according to the dose schedules indicated. Tumor regression (T/C %) on day 14 was determined.

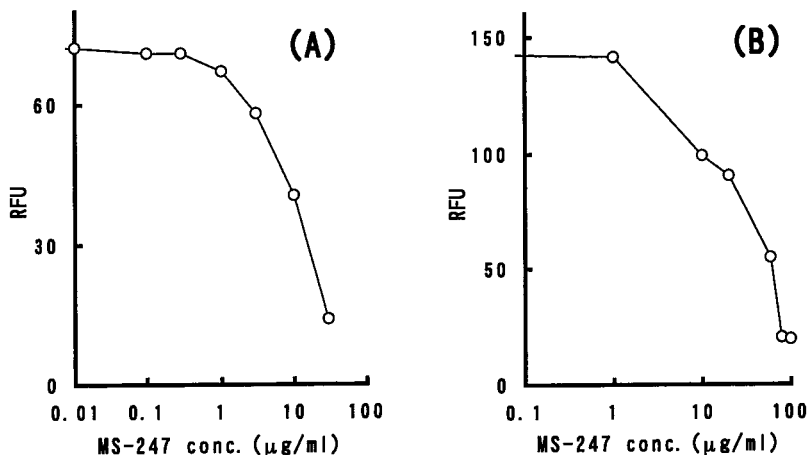
Drug dose (mg/kg) ^a schedule ^b	T/C (%)								
	MS247 25 qd \times 1	Cisplatin 10 qd \times 1	Paclitaxel 28 qd \times 5	CPT-11 100 q4d \times 3	ADM 12 qd \times 1	5-Fu 50 q4d \times 3	CPM 260 qd \times 1	VP-16 12 qd \times 5	VCR 1.6 qd \times 1
Lung cancer									
NCI-H23	4 ^c	10 ^c	4 ^c	8 ^c	43 ^c	63	21 ^c	67	67
NCI-H226	29 ^c	71	6 ^c	14 ^c	40 ^c	70	89	78	24 ^c
NCI-H460	32 ^c	45 ^c	22 ^c	35 ^c	45 ^c	41	60	66	81
A 549	50 ^c	78	29 ^c	75	78	111	88	76	73
DMS 114	19 ^c	69	27 ^c	20 ^c	52	63	9 ^c	61	20 ^c
DMS 273	2 ^c	33 ^c	1 ^c	5 ^c	71	70	43 ^c	137	27 ^c
Stomach cancer									
MKN-1	42 ^c	63	46 ^c	49 ^c	41	55	74	103	88
MKN-7	32 ^c	60	11 ^c	41 ^c	58	75	79	68	66
MKN-74	35 ^c	78	16 ^c	28 ^c	78	76	69	134	82
St-4	24 ^c	62	22 ^c	42 ^c	66	55	95	86	87
Colon cancer									
HCC-2998	28 ^c	52	1 ^c	16 ^c	72	42	71	76	73
HCT-1116	30 ^c	78	5 ^c	11 ^c	60	48 ^c	53	64	57
HCT-15	46 ^c	54	78	10 ^c	73	61	53	66	104
Breast cancer									
HBC-4	24 ^c	56	37 ^c	54	46 ^c	49 ^c	41 ^c	86	46 ^c
MDA-MB-231	18 ^c	28 ^c	13 ^c	50 ^c	86	83	25 ^c	56	32 ^c
Ovarian cancer									
SK-OV-3	39 ^c	72	45 ^c	80	53	75	105	100	85
OVCR-8	36 ^c	69	17 ^c	18 ^c	58	76	78	74	80
Positive rate	17/17	4/17	16/17	14/17	4/17	2/17	5/17	0/17	5/17

^a Each drug was administered at MTD in the schedule indicated.

^b The administration schedules were abbreviated as: qd \times 1, a single injection; qd \times 5, five daily injections; q4d \times 3, 3 injections with a 4-day interval.

^c $P < 0.01$ by Mann Whitney U test as compared with respective control.

Fig. 5. Quenching of the fluorescence of DNA-bound Hoechst 33342 by MS-247. The fluorescence of DNA-bound Hoechst 33342 was measured under the following conditions: A, calf thymus DNA was preincubated with Hoechst 33342 and then incubated with MS-247; B, L1210 cells were preincubated with Hoechst 33342 and then incubated with MS-247. The fluorescence derived from DNA-bound Hoechst 33342 decayed when MS-247 was added to the two systems.



shown in Fig. 8, MS-247 at concentrations around IC_{50} induced a DNA ladder in HL-60 cells. These results demonstrated that MS-247 induced apoptosis.

DISCUSSION

MS-247 is a synthetic compound with a netropsin-like moiety and an alkylating residue in its structure. We found MS-247 by screening about 300 similar compounds, based primarily on the activity of tumor cell growth inhibition, and selected MS-247 for extensive evaluation because of its significant antitumor activity against murine tumors, L1210 and colon 26, and its higher stability.⁴

In the present study, we evaluated the antitumor activity of MS-247 by an *in vitro* and *in vivo* human cancer cell line panel. The mean log GI_{50} of MS-247 was -6.15 ($0.71 \mu M$), which fell in the middle of the range of anticancer drugs presently in use. The COMPARE analysis indicated that the differential growth inhibition pattern of MS-247 (the mean graph) significantly correlated with those of camptothecin analogues and anthracyclins, suggesting that the modes of action are similar. The most remarkable feature of MS-247 was its efficacy

against human xenografts. A single 25 mg/kg injection of MS-247 showed significant antitumor activity against all 17 xenografts tested, which included lung, colon, stomach, breast, and ovarian cancers. In comparison with the clinically active drugs, MS-247 was more effective than cisplatin, ADM, 5-FU, CPM, VP-16, and VCR, in most cases, and moreover, was almost comparable with paclitaxel and CPT-11, the most clinically promising drugs at the present. These results demonstrated the broad anticancer spectrum of MS-247. It is noticeable that MS-247 was more effective than paclitaxel in HCT-15 and than CPT-11 in A549, HBC-4, and SK-OV-3. On the other hand, the toxicity of MS-247, indicated by the body weight loss, was reversible within 10 days after the administration. In our preliminary study, the dose-limiting toxicity of MS-247 was bone marrow suppression. Our results suggest that MS-247 is a promising anticancer drug candidate for further research and development toward clinical investigation.

We also investigated the mode of action of MS-247. We confirmed its binding to DNA by the fact that MS-247 displaced DNA-bound Hoechst 33342 both in the cell-free system and in the cellular system. Hoechst 33342 is a fluorochrome that binds to AT-rich sites in the DNA minor groove and covers four bp, AATT (31, 32). Therefore, it seems correct to consider MS-247 as a DNA minor groove binder, as expected, and that it shares sequence specificity at least with Hoechst 33342.

MS-247 proved to have inhibitory activity against topoisomerases I and II. This was reasonable to expect because several DNA minor groove binders reportedly inhibit topoisomerases. For example, Hoechst 33342, Hoechst 33258, distamycin A, berenil, netropsin, and tallimustine inhibited topoisomerase I (33–35), and distamycin A and tallimustine inhibited topoisomerase II (34, 36). The inhibitory activity against topoisomerase I and II was also expected because the results of the COMPARE analysis suggested that the mode of action of MS-247 was similar to those of camptothecin analogues (topoisomerase I inhibitors) and anthracyclins (topoisomerase II inhibitors). Therefore, topoisomerases I and II are at least the molecular targets of MS-247. Moreover, there might be other possible targets, such as other enzymes, involved in DNA metabolism and/or transcription factors because their activities were inhibited by some DNA minor groove binders (34, 37, 38).

MS-247 blocked the cell cycle at the G_2 -M phase and induced apoptosis. The G_2 -M blockage is the common feature of DNA minor groove binders (1, 39). However, subsequent induction of apoptosis by this type of drug has not been studied, except for apoptosis induced by Hoechst 33342 (40, 41). We showed here the induction of apoptosis by MS-247, which possibly contributes to *in vivo* efficacy, at

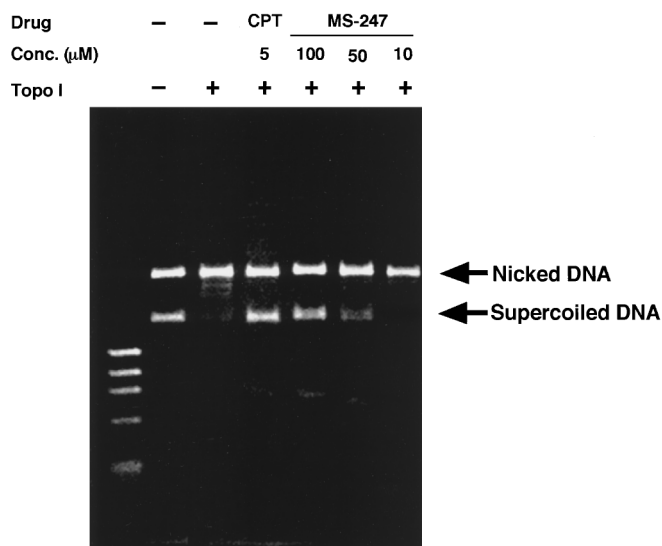


Fig. 6. Inhibition of topoisomerase I by MS-247. Supercoiled DNA was mixed with an indicated concentration of MS-247 or camptothecin before topoisomerase I was added. After a 30-min incubation at 37°C, the reaction mixture was treated as described in "Materials and Methods," and the DNA was analyzed by 1% agarose gel electrophoresis. MS-247 inhibited the topoisomerase I-induced DNA relaxation at concentrations of 50 and 100 μM . Camptothecin was used as a positive control.

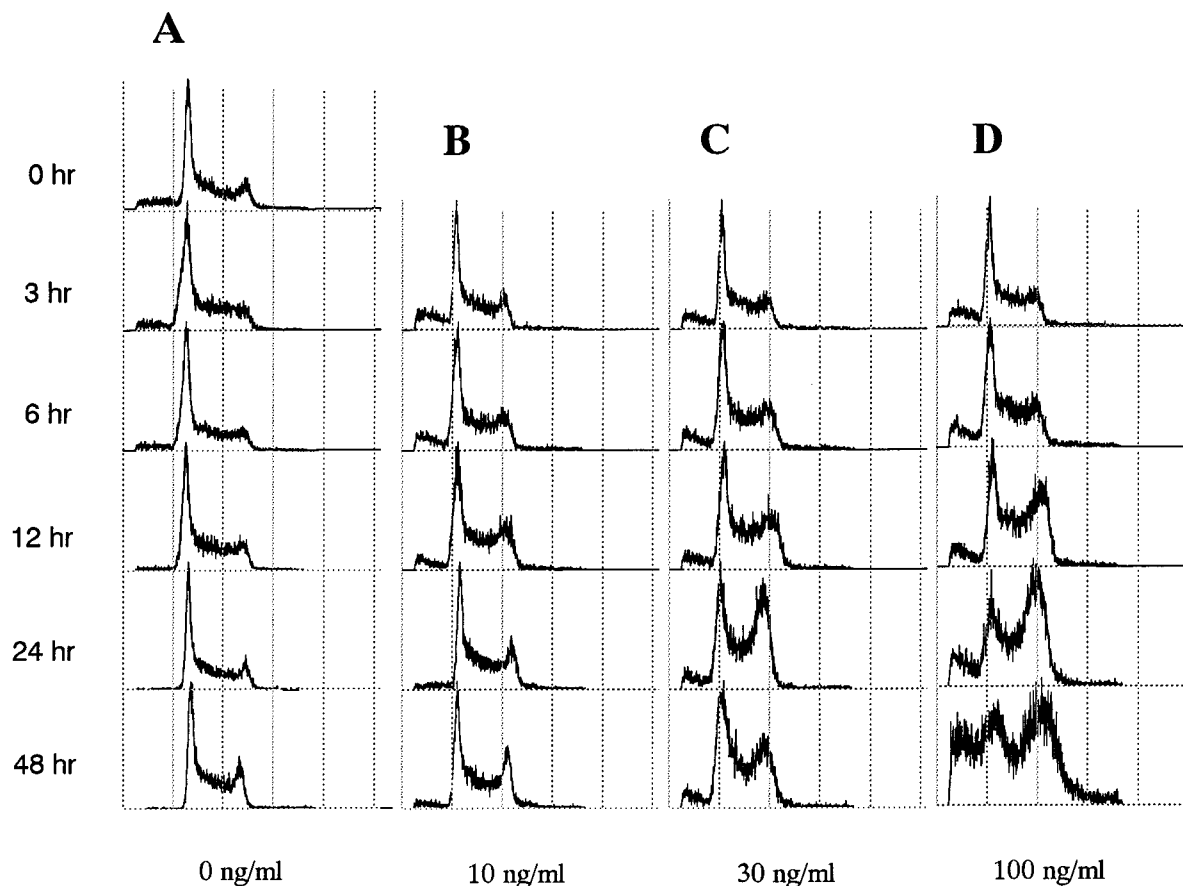


Fig. 7. Effect of MS-247 on cell cycle. L1210 cells were exposed to 0 (A), 10 (B), 30 (C), and 100 ng/ml (D) of MS-247 for 3–48 h. Then, the DNA content of the cells was analyzed by a flow cytometer as described in "Materials and Methods." When exposed to MS-247, the cell population in the G₂-M phase significantly increased.

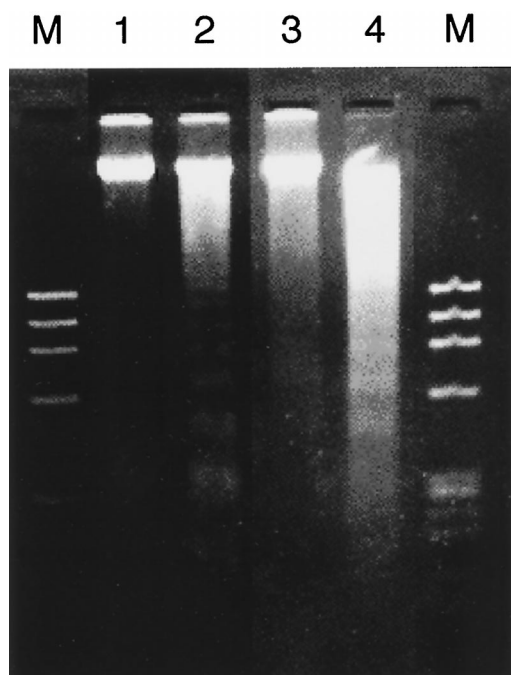


Fig. 8. Apoptosis induced by MS-247. Total DNA was extracted from HL-60 cells treated with nothing (Lane 1), 2 μ M MS-247 (Lane 2), 0.2 μ M MS-247 (Lane 3), or 20 nM camptothecin (Lane 4). Then, DNA fragmentation was measured by electrophoresis, as described in "Materials and Methods." Camptothecin was used as a positive control. Lane M, DNA size markers (ϕ x174/HaeIII).

least in part. Recently, the analysis of the apoptotic cascade induced by anticancer drugs has been studied (42). It seems an important next step to analyze the mechanism of apoptosis induced by MS-247 and to compare MS-247 with other antitumor agents.

Tallimustine, a derivative of distamycin A, has the closest structural relationship to MS-247 of the DNA minor groove binders that were developed as anticancer drugs. Although tallimustine was subjected to clinical trials, its efficacy has not yet been demonstrated (17, 18). It may be important to compare MS-247 and tallimustine in a preclinical study. In our preliminary study, the sequence specificity of DNA binding between the two is slightly different, suggesting that MS-247 is different from tallimustine in biological activity.

We report here our synthesis of a novel DNA minor groove binder, MS-247, and have demonstrated its strong antitumor activity against several human cancer xenografts. We see that MS-247 binds to DNA, inhibits topoisomerases and other possible targets around DNA, blocks the cell cycle at G₂-M, and induces apoptosis. MS-247 is a promising new anticancer drug for further development toward clinical investigation.

ACKNOWLEDGMENTS

We thank Dr. R. H. Shoemaker and Dr. K. D. Paull (Developmental Therapeutics Program, Division of Cancer Treatment, National Cancer Institute) for their helpful discussions during the development of the human cancer cell line panel and the database system.

REFERENCES

1. Turner, P. R., and Denny, W. A. The mutagenic properties of DNA minor-groove binding ligands. *Mutat. Res.*, 355: 141–169, 1996.

2. Hartley, J. A., Lown, J. W., Mattes, W. B., and Kohn, K. W. DNA sequence specificity of antitumor agents. Oncogenes as possible targets for cancer therapy. *Acta. Oncol.*, *27*: 503–510, 1988.
3. Lown, J. W. DNA recognition by lexitropsins, minor groove binding agents. *J. Mol. Recognit.* *7*: 79–88, 1994.
4. Marchini, S., Cozzi, P., Beria, I., Geroni, C., Capolongo, L., D'Incalci, M., and Broggin, M. Sequence-specific DNA alkylation of novel tallimustine derivatives. *Anticancer Drug Des.*, *13*: 193–205, 1998.
5. Brooks, N., Lee, M., Wright, S. R., Woo, S., Centioni, S., and Hartley, J. A. Synthesis, DNA binding, cytotoxicity and sequence specificity of a series of imidazole-containing analogs of the benzoic acid mustard distamycin derivative tallimustine containing an alkylating group at the C-terminus. *Anticancer Drug Des.*, *12*: 591–606, 1997.
6. Yoon, J. H., and Lee, C. S. Sequence selectivity of DNA alkylation by adozelesin and carzelesin. *Arch. Pharmacol. Res. (Seoul)*, *21*: 385–390, 1998.
7. Bhuyan, B. K., Smith, K. S., Adams, E. G., Wallace, T. L., Von Hoff, D. D., and Li, L. H. Adozelesin, a potent new alkylating agent: cell-killing kinetics and cell-cycle effects. *Cancer Chemother. Pharmacol.*, *30*: 348–354, 1992.
8. Burris, H. A., Dieras, V. C., Tunca, M., Earhart, R. H., Eckardt, J. R., Rodriguez, G. I., Shaffer, D. S., Fields, S. M., Campbell, E., Schaaf, L., Kasunic, D., and Von Hoff, D. D. Phase I study with the DNA sequence-selective agent adozelesin. *Anticancer Drugs*, *8*: 588–596, 1997.
9. Foster, B. J., LoRusso, P. M., Poplin, E., Zalupski, M., Valdivieso, M., Wozniak, A., Flaherty, L., Kasunic, D. A., Earhart, R. H., and Baker, L. H. Phase I trial of adozelesin using the treatment schedule of daily $\times 5$ every 3 weeks. *Invest. New Drugs*, *13*: 321–326, 1996.
10. Li, L. H., DeKoning, T. F., Kelly, R. C., Krueger, W. C., McGovern, J. P., Padbury, G. E., Petzold, G. L., Wallace, T. L., Ouding, R. J., Prairie, M. D., and Gebhard, I. Cytotoxicity and antitumor activity of carzelesin, a prodrug cyclopropylpyrroloindole analogue. *Cancer Res.*, *52*: 4904–4913, 1992.
11. Houghton, P. J., Cheshire, P. J., Hallman, J. D. N., and Houghton, J. A. Therapeutic efficacy of the cyclopropylpyrroloindole, carzelesin, against xenografts derived from adult and childhood solid tumors. *Cancer Chemother. Pharmacol.*, *36*: 45–52, 1995.
12. Carter, C. A., Waud, W. R., Li, L. H., DeKoning, T. F., McGovern, J. P., and Plowman, J. Preclinical antitumor activity of bizelesin in mice. *Clin. Cancer Res.*, *2*: 1143–1149, 1996.
13. Walker, D. L., Reid, J. M., and Ames, M. M. Preclinical pharmacology of bizelesin, a potent bifunctional analog of the DNA-binding antibiotic CC-1065. *Cancer Chemother. Pharmacol.*, *34*: 317–322, 1994.
14. Kobayashi, E., Okamoto, A., Asada, M., Okabe, M., Nagamura, S., Asai, A., Saito, H., Gomi, K., and Hirata, T. Characteristics of antitumor activity of KW-2189, a novel water-soluble derivative of duocarmycin, against murine and human tumors. *Cancer Res.*, *54*: 2404–2410, 1994.
15. Pezzoni, G., Grandi, M., Biasoli, G., Capolongo, L., Ballinari, D., Giuliani, F. C., Barbieri, B., Pastori, A., Pesenti, E., Mongelli, N., and Spreafico, F. Biological profile of FCE 24517, a novel benzoyl mustard analogue of distamycin A. *Br. J. Cancer*, *64*: 1047–1050, 1991.
16. Verweij, J. New promising anticancer agents in development: what comes next? *Cancer Chemother. Pharmacol.*, *38* (Suppl.): S3–S10, 1996.
17. Viallet, J., Stewart, D., Shepherd, F., Ayoub, J., Cormier, Y., DiPietro, N., and Steward, W. Tallimustine is inactive in patients with previously treated small cell lung cancer. A Phase II trial of the National Cancer Institute of Canada Clinical Trials Group. *Lung Cancer*, *15*: 367–373, 1996.
18. Punt, C. J., Humblet, Y., Roca, E., Dirix, L. Y., Wainstein, R., Polli, A., and Corradino, I. Tallimustine in advanced previously untreated colorectal cancer, a Phase II study. *Br. J. Cancer*, *73*: 803–804, 1996.
19. Alberts, S. R., Erlichman, C., Reid, J. M., Sloan, J. A., Ames, M. M., Richardson, R. L., and Goldberg, R. M. Phase I study of the duocarmycin semisynthetic derivative KW-2189 given daily for five days every six weeks. *Clin. Cancer Res.*, *4*: 2111–2117, 1998.
20. Taberero, L., Verdager, N., Coll, M., Fita, I., van der Marel, G. A., van Boom, J. H., Rich, A., and Aymami, J. Molecular structure of the A-tract DNA dodecamer d(CGCAAATTTGCG) complexed with the minor groove binding drug netropsin. *Biochemistry*, *32*: 8403–8410, 1993.
21. Stinson, S. F., Alley, M. C., Kopp, W. C., Fiebig, H. H., Mullendore, L. A., Pittman, A. F., Kenney, S., Keller, J., and Boyd, M. R. Morphological and immunocytochemical characteristics of human tumor cell lines for use in a disease-oriented anticancer drug screen. *Anticancer Res.*, *12*: 1035–1053, 1992.
22. Satoh, A., Takayama, E., Kojima, K., Ogawa, H., Yamori, T., Sato, S., Kawaguchi, T., Tsuruo, T., Yoshimoto, K., Kine, T., and Matsumoto, I. Expression of carbohydrate-binding protein p33/41 human tumor cell lines. *J. Biochem.*, *119*: 346–353, 1996.
23. Motoyama, T., Hojo, H., and Watanabe, H. Comparison of seven cell lines derived from human gastric carcinomas. *Acta. Pathol. Jpn.*, *36*: 65–83, 1986.
24. Boyd, M. R. Status of the National Cancer Institute preclinical antitumor drug discovery screen: implications for selection of new agents for clinical trial. In: V. T. Devita, Jr., S. Hellman, and S. A. Rosenberg (eds.), *Cancer: Principles and Practice of Oncology Update*, Vol. 3, pp. 1–12. Philadelphia: Lippincott, 1989.
25. Paull, K. D., Shoemaker, R. H., Hodes, L., Monks, A., Scudiero, D. A., Rubinstein, L., Plowman, J., and Boyd, M. R. Display and analysis of patterns of differential activity of drugs against human tumor cell lines: development of mean graph and COMPARE algorithm. *J. Natl. Cancer Inst.*, *81*: 1088–1092, 1989.
26. Monks, A., Scudiero, D., Skehan, P., Shoemaker, R., Paull, K., Vistica, D., Hose, C., Langley, J., Cronise, P., Vaigro-Wolf, A., Gray-Goodrich, M., Campbell, H., Mayo, J., and Boyd, M. Feasibility of a high-flux anticancer drug screen using a diverse panel of cultured human tumor cell lines. *J. Natl. Cancer Inst.*, *83*: 757–766, 1991.
27. Yamori, T., Sato, S., Chikazawa, H., and Kadota, T. Anti-tumor efficacy of paclitaxel against human lung cancer xenografts. *Jpn. J. Cancer Res.*, *88*: 1205–1210, 1997.
28. Skehan, P., Storeng, R., Scudiero, D., Monks, A., McMahon, J., Vistica, D., Warren, J. T., Bokesch, H., Kenney, S., and Boyd, M. R. New colorimetric cytotoxicity assay for anticancer-drug screening. *J. Natl. Cancer Inst.*, *82*: 1107–1112, 1990.
29. Goldwasser, F., Shimizu, T., Jackman, J., Hoki, Y., O'Connor, P. M., Kohn, K. W., and Pommier, Y. Correlations between S and G2 arrest and the cytotoxicity of camptothecin in human colon carcinoma cells. *Cancer Res.*, *56*: 4430–4437, 1996.
30. Ishizawa, M., Kobayashi, Y., Miyamura, T., and Matsuura, S. Simple procedure of DNA isolation from human serum. *Nucleic Acids Res.*, *19*: 5792, 1991.
31. Sriram, M., van der Marel, G. A., Roelen, H. L., van Boom, J. H., and Wang, A. H. Conformation of B-DNA containing O⁶-ethyl-G-C base pairs stabilized by minor groove binding drugs: molecular structure of d(CGC[e6G]AATTCGCG) complexed with Hoechst 33258 or Hoechst 33342. *EMBO J.*, *11*: 225–232, 1992.
32. Robinson, H., Gao, Y. G., Bauer, C., Roberts, C., Switzer, C., and Wang, A. H. 2'-Deoxyisoguanosine adopts more than one tautomer to form base pairs with thymidine observed by high-resolution crystal structure analysis. *Biochemistry*, *37*: 10897–10905, 1998.
33. Chen, A. Y., Yu, C., Gatto, B., and Liu, L. F. DNA minor groove-binding ligands: a different class of mammalian DNA topoisomerase I inhibitors. *Proc. Natl. Acad. Sci. USA*, *90*: 8131–8135, 1993.
34. Montecucco, A., Fontana, M., Focher, F., Lestingi, M., Spadari, S., and Ciarrocchi, G. Specific inhibition of human DNA ligase adenylation by a distamycin derivative possessing antitumor activity. *Nucleic Acids Res.*, *19*: 1067–1072, 1991.
35. Wang, Z., Zimmer, C., Lown, J. W., and Knippers, R. Effects of bifunctional netropsin-related minor groove-binding ligands on mammalian type I DNA topoisomerase. *Biochem. Pharmacol.*, *53*: 309–316, 1997.
36. Fesen, M., and Pommier, Y. Mammalian topoisomerase II activity is modulated by the DNA minor groove binder distamycin in simian virus 40 DNA. *J. Biol. Chem.*, *264*: 11354–11359, 1989.
37. Bellorini, M., Moncollin, V., D'Incalci, M., Mongelli, N., and Mantovani, R. Distamycin A and tallimustine inhibit TBP binding and basal *in vitro* transcription. *Nucleic Acids Res.*, *23*: 1657–1663, 1995.
38. Broggin, M., and D'Incalci, M. Modulation of transcription factor–DNA interactions by anticancer drugs. *Anticancer Drug Des.*, *9*: 373–387, 1994.
39. Erba, E., Mascellani, E., Pifferi, A., and D'Incalci, M. Comparison of cell-cycle phase perturbations induced by the DNA-minor-groove alkylator tallimustine and by melphalan in the SW626 cell line. *Int. J. Cancer*, *62*: 170–175, 1995.
40. Zhang, X., and Kiechle, F. L. Hoechst 33342 induces apoptosis and alters TATA box binding protein/DNA complexes in nuclei from BC3H-1 myocytes. *Biochem. Biophys. Res. Commun.*, *248*: 18–21, 1998.
41. Zhang, X., and Kiechle, F. L. Mechanism of Hoechst 33342-induced apoptosis in BC3H-1 myocytes. *Ann. Clin. Lab. Sci.*, *28*: 104–114, 1998.
42. Kamesaki, H. Mechanisms involved in chemotherapy-induced apoptosis and their implications in cancer chemotherapy. *Int. J. Hematol.*, *68*: 29–43, 1998.

Cancer Research

The Journal of Cancer Research (1916–1930) | The American Journal of Cancer (1931–1940)

Potent Antitumor Activity of MS-247, a Novel DNA Minor Groove Binder, Evaluated by an *in Vitro* and *in Vivo* Human Cancer Cell Line Panel

Takao Yamori, Akio Matsunaga, Shigeo Sato, et al.

Cancer Res 1999;59:4042-4049.

Updated version Access the most recent version of this article at:
<http://cancerres.aacrjournals.org/content/59/16/4042>

Cited articles This article cites 40 articles, 8 of which you can access for free at:
<http://cancerres.aacrjournals.org/content/59/16/4042.full#ref-list-1>

Citing articles This article has been cited by 16 HighWire-hosted articles. Access the articles at:
<http://cancerres.aacrjournals.org/content/59/16/4042.full#related-urls>

E-mail alerts [Sign up to receive free email-alerts](#) related to this article or journal.

Reprints and Subscriptions To order reprints of this article or to subscribe to the journal, contact the AACR Publications Department at pubs@aacr.org.

Permissions To request permission to re-use all or part of this article, use this link
<http://cancerres.aacrjournals.org/content/59/16/4042>.
Click on "Request Permissions" which will take you to the Copyright Clearance Center's (CCC) Rightslink site.